Early endosomes and endosomal coatomer are required for autophagy

Minoo Razi, Edmond Y.W. Chan, and Sharon A. Tooze

London Research Institute, Cancer Research UK, London WC2A 3PX, England, UK

Autophagy, an intracellular degradative pathway, maintains cell homeostasis under normal and stress conditions. Nascent double-membrane autophagosomes sequester and enclose cytosolic components and organelles, and subsequently fuse with the endosomal pathway allowing content degradation. Autophagy requires fusion of autophagosomes with late endosomes, but it is not known if fusion with early endosomes is essential. We show that fusion of AVs with functional early endosomes is required for autophagy. Inhibition of early endosome function by loss of COPI subunits (β′, β, or α) results in accumulation of autophagosomes, but not an increased autophagic flux. COPI is required for ER-Golgi transport and early endosome maturation. Although loss of COPI results in the fragmentation of the Golgi, this does not induce the formation of autophagosomes. Loss of COPI causes defects in early endosome function, as both transferrin recycling and EGF internalization and degradation are impaired, and this loss of function causes an inhibition of autophagy, an accumulation of p62/SQSTM-1, and ubiquitinated proteins in autophagosomes.

Introduction

Macroautophagy, here referred to as autophagy, is a highly conserved degradative process used for the nonselective removal of long-lived proteins, large protein aggregates, and subcellular organelles. In contrast, selective forms of autophagy, such as pexophagy and mitophagy, and chaperone-mediated autophagy, target specific substrates and organelles for degradation (Mizushima et al., 2008). Successful autophagy of all types requires a response to an initiation signal, for example starvation, followed by the expansion of the autophagosomal membrane source, a double membrane called an isolation membrane or phagophore. The isolation membrane efficiently sequesters subcellular components and forms the nascent, or immature, autophagosome or autophagic vacuole (AVi), which fuses with endosomes and lysosomes to acquire proteases and lipases. Fusion of AVi with endosomes and lysosomes results in the formation of amphisomes (AVi/d) and autolysosomes, or degradative AVs (AVd).

Autophagy requires a set of proteins called the Atg (autophagy related) proteins, first identified in yeast (Klionsky, 2007). Mammalian orthologues of many of the 31 yeast Atg proteins have been identified and characterized, and it is through the work in yeast and mammals that the role of many of these proteins is beginning to be understood. Early stages of AV formation requires ULK1, the orthologue of the Atg1 kinase, the PtdIns-3 kinase Vps34, and two ubiquitin-like conjugation systems, whose actions result in formation of the Atg5-12-16 complex, and LC3-II. LC3-II is the lipid-conjugated form of LC3-I, an orthologue of yeast Atg8, and the most widely used marker of AVs. This core machinery drives the initiation, expansion, and closure of the isolation membrane (Xie and Klionsky, 2007).

The final stages of AV maturation, the formation of AVi/ds and AVds, occurs through fusion with endosomes and lysosomes, in particular multi-vesicular bodies (MVB) (Filimonenko et al., 2007), which are formed from early endosomes by the ESCRT machinery (Williams and Urbe, 2007; Woodman and Futter, 2008). Recently, the ESCRT complexes were shown to be required for formation of autolysosomes; loss of Tsg101 (ESCRTI) or Vps24 (ESCRTIII) results in an accumulation of amphisomes (Filimonenko et al., 2007). Furthermore, the loss or mutation of several components of the ESCRT machinery, in

Correspondence to Sharon A. Tooze: sharon.tooze@cancer.org.uk

E.Y.W. Chan's present address is Strathclyde Institute of Pharmacy and Biomedical Sciences, University of Strathclyde, Glasgow G4 0NR, Scotland, UK.

Abbreviations used in this paper: ARF, ADP-ribosylation factor; Atg, autophagy related; AV, autophagic vacuole; COP, coat protein complex; EEA1, early endosomal autoantigen 1; ERGIC-53, ER-Golgi intermediate compartment 53 kD; GM130, Golgi membrane protein 130 kD; LAMP, lysosomal-associated membrane protein; LTR, Lysotracker red; MPR, mannose-6-phosphate receptor; MVB, multi-vesicular body; Tfn, transferrin; Ub, ubiquitin.

The Rockefeller University Press $30.00
J. Cell Biol. Vol. 185 No. 2 305–321
www.jcb.org/cgi/doi/10.1083/jcb.200810098

particular ESCRT0 (Hrs), ESCRTI (Tsg101), and ESCRTIII (CHMP2B) results in neurodegeneration caused by an accumulation of ubiquitinated intracellular aggregates and abnormal AVs (Filimonenko et al., 2007; Kim et al., 2007; Lee et al., 2007). However, it has been previously suggested that AV maturation occurs by a multi-step, sequential fusion of AVs with different populations of early and late endosomes, and lysosomes (Dunn, 1990; Eskelinen, 2005). Indeed, there is evidence that early endosomes fuse with AVis (Gordon and Seglen, 1988; Tooze et al., 1990; Liou et al., 1997), but it is not known if this fusion is obligatory for autophagy.

Maintenance of endosomal/lysosomal function has also been shown to depend on coatomer subunits α-, β-, and ε-COP (Whitney et al., 1995; Guo et al., 1996; Daro et al., 1997; Gu et al., 1997; Styers et al., 2008), although the best-characterized role of COPI vesicles is in vesicular transport between the Golgi complex and ER (Lee et al., 2004). Coatomer is composed of seven subunits, found in two subcomplexes, F-COPI (β, γ, δ, ζ) and B-COPI (β′, α, ε) (Eugster et al., 2000), which associate with membranes via ARF (ADP-ribosylation factor), a small GTPase, and the p24 proteins (Nickel et al., 2002).

We found that depletion of β′-, β-, or α-COP results in an accumulation of AVis and AVi/ds, and demonstrate this occurs because of an impairment of early endosomes. Specifically, our data show that the loss of COPI function impairs transport into and through early endosomes, and this impairment causes an accumulation of GFP-LC3–positive AVs and a block in AV maturation, which leads to an inhibition of autophagic flux. Our results provide direct evidence that fusion of AVis with early endosomes is required for autophagy.

Results

β′-COP depletion increases GFP-LC3 lipidation and GFP-LC3–positive structures

During an siRNA screen with the Dharmacon 700-member kinome library for modulators of autophagy (Chan et al., 2007), we found that depletion of PKC-ε RACK (receptors for activated C-kinase) (Csukai et al., 1997) resulted in a threefold increase of lipidated GFP-LC3 (GFP-LC3-II) in fed cells compared with the siRNA control. Induction of autophagy is monitored by the conversion of GFP-LC3-I to GFP-LC3-II, which is detected by immunoblotting as LC3-II migrates faster during SDS-PAGE. As RACK was previously identified as β′-COP (Csukai et al., 1997), and β′-COP is one of seven subunits of the coatomer complex (Eugster et al., 2000), we investigated whether siRNA depletion of the two other subunits to which we had antibodies, β- and α-COP (Fig. 1 A), showed the same increase in GFP-LC3-II.

As seen in Fig. 1 B, depletion of β- and α-COP, like β′-COP, resulted in a significant increase in GFP-LC3-II in HEK293A cells stably expressing GFP-LC3 (293/GFP-LC3 cells). In addition, after depletion of β′-, β-, and α-COP in 293/GFP-LC3 cells there was a large increase in the number of GFP-LC3–positive punctate structures (Fig. 1 C). Identical results with LC3 were obtained in HEK293A parental cells and HeLa cells (not depicted). These results demonstrated that loss of coatomer subunits β′-, β-, and α-COP increased GFP-LC3-II and the number of GFP-LC3-II–positive vesicles, and suggested a role for COPI in autophagy.

As a control for the specificity of COP depletion we tested if siRNA knockdown of the other coat complexes involved in transport between the ER and Golgi, such as COPII subunits, caused an increase in GFP-LC3-II, or GFP-LC3–positive vesicles under the same culture conditions. 293/GFP-LC3 cells treated with siRNAs for COPII subunits Sec23A and 23B (Fig. 1 A) or Sec31 (not depicted) showed no increase in GFP-LC3-II (Fig. 1 B), or GFP-LC3–positive vesicles (not depicted). The lack of increase in lipidated GFP-LC3 and GFP-positive puncta after depletion of COPII indicated that the effect was specific to COPI, and suggested that it was not a result of a general inhibition of ER-to-Golgi transport.

Golgi disassembly occurs before but does not induce GFP-LC3 lipidation or vesicle formation

Depletion of β-COP has been shown to cause a collapse of the ER, ERGIC, and Golgi complex into a large globular compartment containing ERGIC-53 (ER-Golgi intermediate compartment) and GM130 (Golgi membrane protein 130 kD) (Styers et al., 2008). Therefore, to study the relationship between the morphological changes of the Golgi complex, GFP-LC3 lipidation, and puncta formation, we performed a time course after siRNA depletion of β′-, β-, and α-COP, and monitored GFP-LC3 and the localization of GM130. After 24 h of siRNA treatment we saw a decrease in the level of both β′- and α-COP (Fig. 2 A), and a subtle change in the distribution of GM130 from a reticular network to a more compact vesiculated structure (Fig. 2 C). After 48 h, in the siRNA-depleted cells GM130 was redistributed and was almost undetectable in most cells (Fig. 2 E). Using transmission electron microscopy (TEM) we observed a vesiculation of the Golgi cisternae and the appearance of numerous small vesicles in the juxta-nuclear region (see Fig. S1), confirming a disruption of the Golgi complex. This result was anticipated given the role of COPI in trafficking from the preGolgi VTCs (vesicular tubular compartments) to and through the Golgi complex (Lee et al., 2004). However, the change in GM130 distribution preceded the appearance of GFP-LC3–positive structures and increases in GFP-LC3-II (Fig. 2 B). After 24 h siRNA depletion of β′-COP (Fig. 2, B and C) there was no detectable GFP-LC3-II, and very few GFP-LC3 puncta were observed, whereas at 48 h (Fig. 2, B and E) there was a significant increase in both GFP-LC3-II and GFP-LC3 puncta. These results suggested that Golgi fragmentation preceded GFP-LC3-II accumulation and GFP-LC3 puncta formation, and that the accumulation of GFP-LC3 puncta may be a consequence of the loss of the Golgi complex.

We then asked if Golgi fragmentation, by itself, would cause a phenotype similar to that seen after COPI depletion resulting in an accumulation of AVs. To test if disassembly or fragmentation of the Golgi was inducing autophagy we used siRNA-depletion of Rab1a/b as an alternative means to disassemble the Golgi complex (Haas et al., 2007). As shown in Fig. 2 D, in 293/GFP-LC3 cells efficient siRNA knockdown of Rab1a and b was obtained, and as anticipated, Rab1 depletion caused a fragmentation of the Golgi

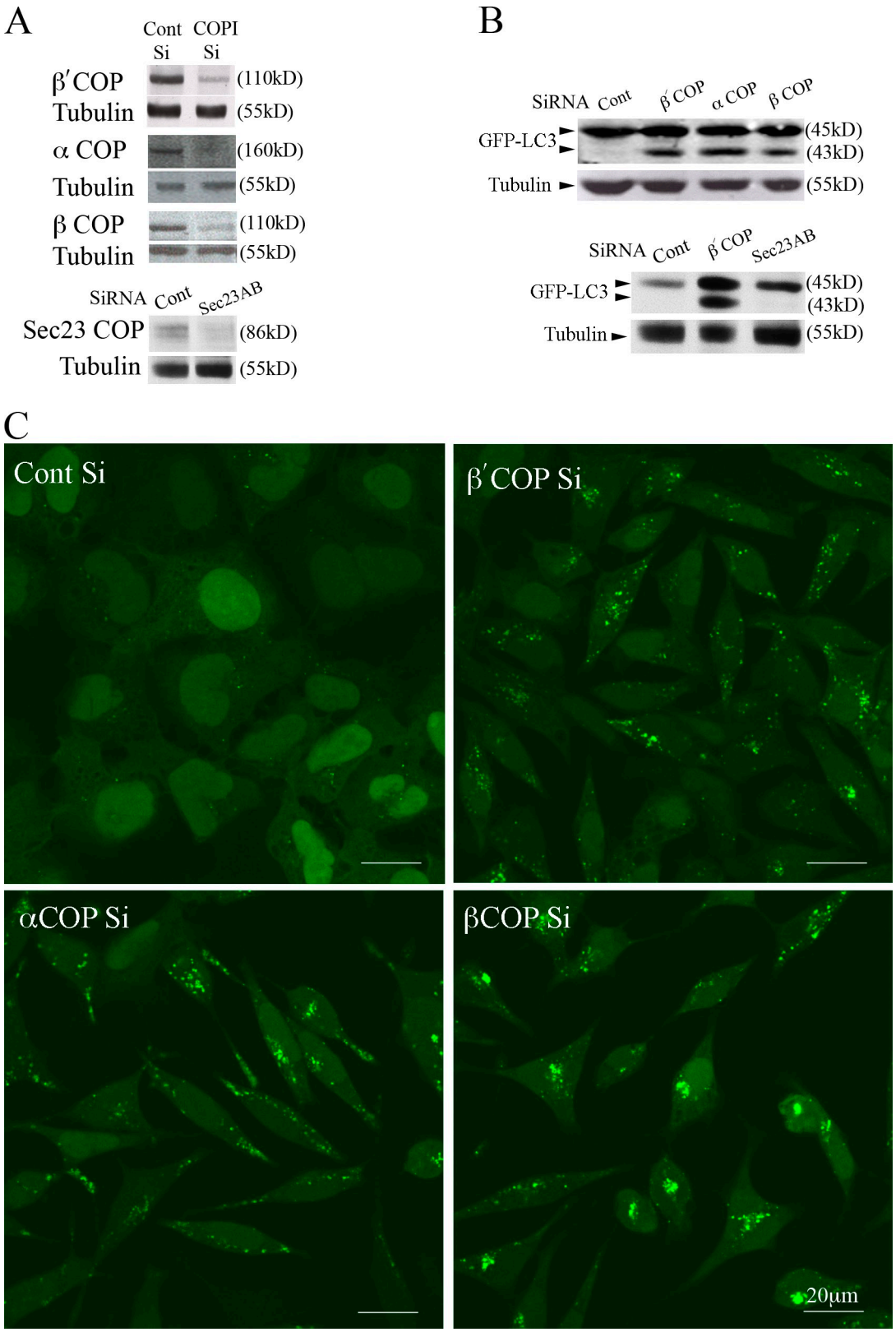

Figure 1. **siRNA depletion of COPI increases autophagy.** (A) siRNA depletion of β′-, β-, and α-COPI (top) and Sec23A and B (bottom) in 293/GFP-LC3 cells for 48 h. Decreased protein levels of the corresponding subunits is shown by immunoblots. (B) Loss of β′-, α-, and β-COP but not subunits of COPII (Sec 23A and B) increase GFP-LC3-II. In A and B, tubulin was the loading control. (C) GFP-LC3–positive vesicles were detectable in 293/GFP-LC3 cells after siRNA depletion of β′-, α-, and β-COP but only basal levels of GFP-LC3–positive vesicles are observed in control siRNA-depleted cells.

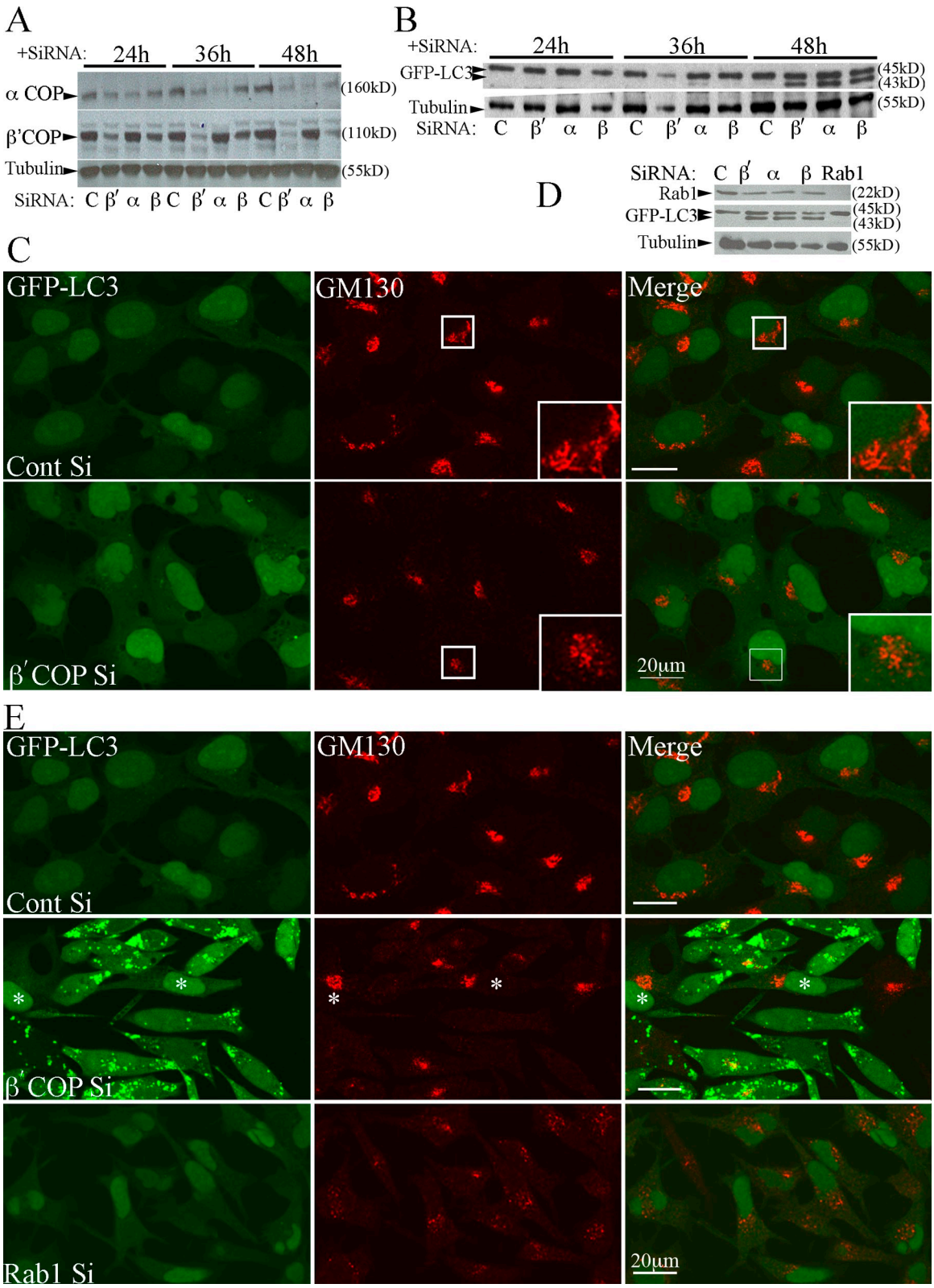

Figure 2. **Time course of COPI depletion shows that Golgi disperses before AVs are formed, but Golgi dispersal does not cause AV formation.** (A) COPI subunits were depleted in 293/GFP-LC3 cells and analyzed 24, 36, and 48 h after addition of siRNA. Immunoblotting for β′- and α-COP confirms loss of COP subunits. (B) GFP-LC3-I and -II were monitored by immunoblots in parallel lysates using anti-GFP antibodies at the indicated times. (C) After 24 h siRNA treatment, depletion of β′-COP caused morphological changes and a reduction in perinuclear population of GM130. Box indicates enlarged area. (D) Rab1a/b was depleted using siRNAs for 48 h. Lysates were probed with anti-Rab1 to confirm depletion. (E) β′-COP or Rab1a/b were depleted as in D, and analyzed by indirect immunofluorescence using anti-GM130 and GFP fluorescence. In β′-COP panel, the asterisk indicates cells that did not show an accumulation of GFP-LC3–positive AVs.

complex (Fig. 2 E); after 24 h both ERGIC-53 (not depicted) and GM130-positive structures became fragmented; however, even after 48 h of Rab1 depletion there was no detectable increase in GFP-LC3–positive structures in the Rab1 siRNA-depleted cells (Fig. 2 E). Similar data were obtained using a 30-min Brefeldin A treatment, which also fragments the Golgi complex (unpublished data). These results support the conclusion that Golgi fragmentation, by itself, does not induce autophagy or cause an accumulation of GFP-LC3–positive structures. In addition, Rab1 is required for COPII vesicle tethering and COPII cargo selection in the ER (Haas et al., 2007). Overall, our data on Rab1 agrees with the lack of effect on GFP-LC3 lipidation and vesicle formation after depletion of COPII subunits and further support the specificity of COPI function in autophagy

We speculated that the loss of COPI function may cause a "stress" signal in the cell, perhaps due to a disruption of protein transport (Styers et al., 2008), which would induce autophagy. A block of protein transport after siRNA-mediated depletion of GBF-1, a guanine nucleotide-exchange factor (GEF) that activates ARF, but not the related GEFs BIG1 and BIG2, leads to an increase in the unfolded protein response (UPR) (Citterio et al., 2008). As BIG1, 2, and GBF-1 are all required for ARF-mediated COPI vesicle formation, we asked if depletion of COPI subunits caused a UPR. This was also important to address, as a UPR has been shown to induce autophagy (Ogata et al., 2006). To monitor the UPR after depletion of β′-COP for 48 h, we examined the levels of the ER chaperone calreticulin, which has been shown to increase during a UPR. We saw no increases in calreticulin levels (Fig. S2 A). Unaltered calreticulin levels were independently confirmed in a recent publication (Styers et al., 2008). Moreover, the level of ERGIC-53 was decreased after β′-COP depletion, supporting our hypothesis that an UPR is not involved as ERGIC-53 has been shown to increase after induction of an UPR (Nyfeler et al., 2003). Lastly, COPI knock-down cells were treated with salubrinal, a compound that has been shown to protect cells from ER stress by inhibiting eukaryotic translation initiation factor 2 subunit α (eIF2α) dephosphorylation (Boyce et al., 2005). Our results showed that incubation of COPI-depleted cells with salubrinal had no effect on the levels of LC3-II (Fig. S2 B). These three results strongly suggest that COPI depletion does not induce autophagy through an increase in ER stress.

GFP-LC3 lipidation and vesicle formation, but not Golgi fragmentation, requires Atg5 and Atg7

Atg proteins are required for the lipidation of GFP-LC3 and the formation of AVs, and therefore to ask if the GFP-LC3 puncta formed in the COPI-depleted cells occurred via an Atg-dependent pathway we cotransfected cells with COPI siRNAs together with siRNAs specific for Atg5 or Atg7. We had previously shown that depletion of Atg5 and Atg7 in 293/GFP-LC3 cells reduces the amount of LC3-II and GFP-LC3–positive AVs (Chan et al., 2007). Depletion of COPI subunits together with Atg5 or Atg7 decreased the lipidation of GFP-LC3-I induced by COPI depletion (Fig. 3 A). Parallel samples processed for fluorescence microscopy revealed these doubly transfected siRNA-depleted cells lack GFP-LC3–positive AVs; in the absence of

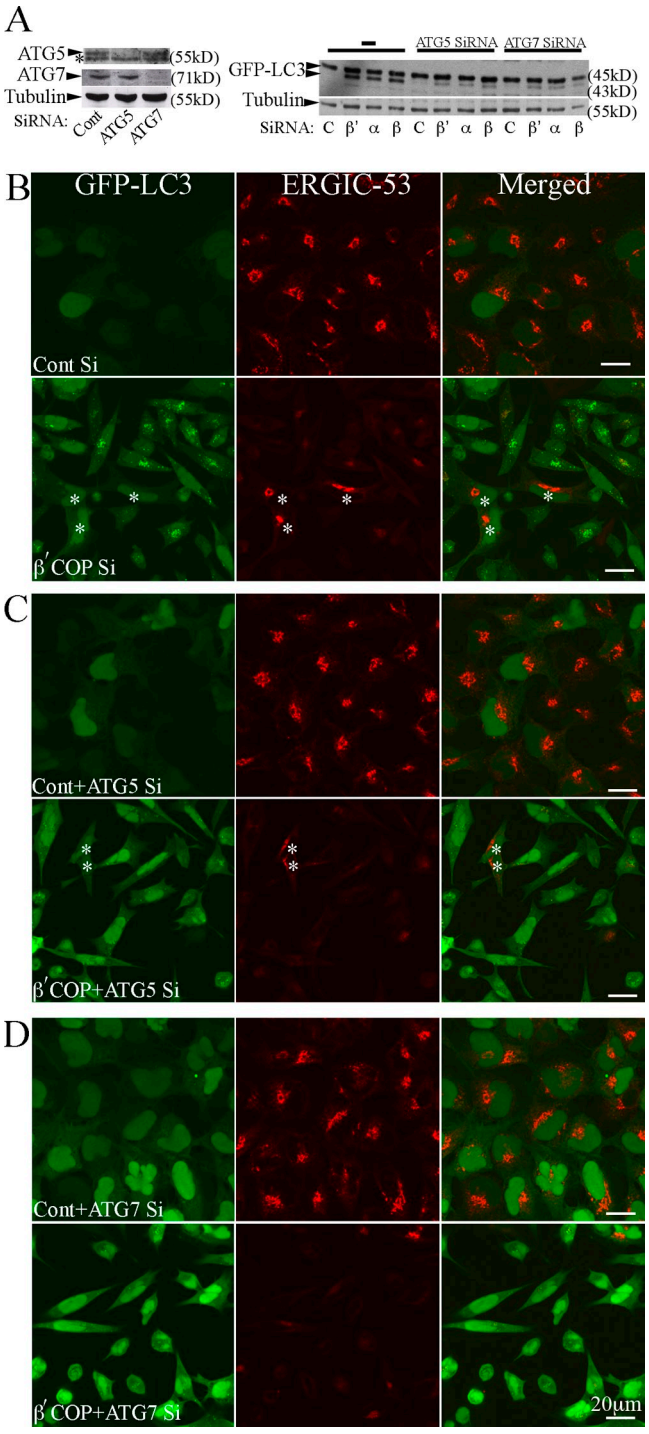

Figure 3. **AV formation after siRNA depletion of COPI requires Atg5 and Atg7.** 293/GFP-LC3 cells were incubated with siRNA for β′-, α-COP, or control siRNA alone or combined with siRNA against Atg5 or Atg7 for 48 h, then (A) lysed and analyzed by immunoblot for Atg5, Atg7, GFP-LC3, and tubulin (loading control), or (B) fixed for immunofluorescence analysis using anti-ERGIC-53 antibodies, or GFP fluorescence. In A, the asterisk indicates nonspecific band; in B and C, asterisk indicates cells that did not show a fragmented ERGIC-53.

Atg5 or Atg7 GFP-LC3 remains diffuse and cytosolic (Fig. 3, C and D), similar to control siRNA-treated cells (Fig. 3 B).

We also asked if the fragmentation and loss of the Golgi complex after COPI depletion was altered in the absence of Atg5

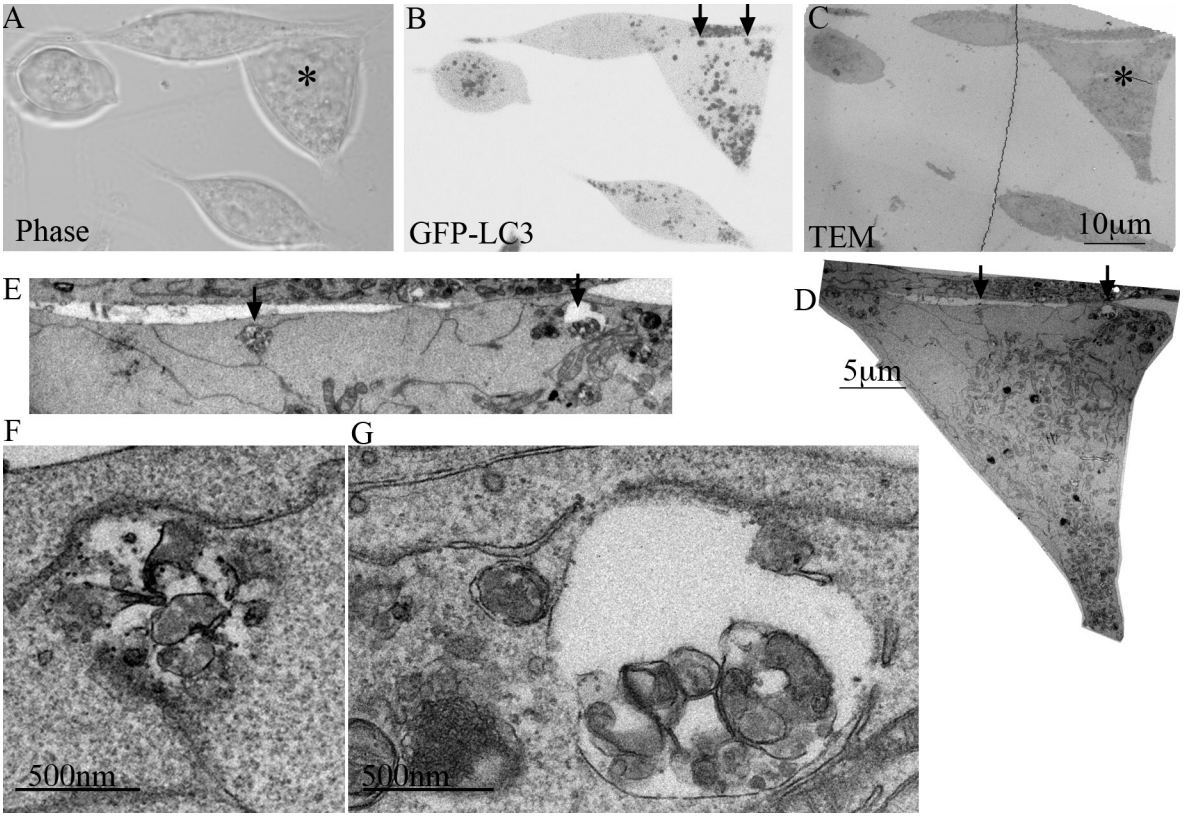

Figure 4. **Correlative light-electron microscopy analysis of GFP-LC3 puncta demonstrates they are AVs.** (A) Phase, (B) fluorescent, and (C) TEM of the same field of 293/GFP-LC3 cells 48 h after siRNA depletion of α-COP. In B the image was inverted to allow better visualization of the GFP-LC3–positive structures. (D) Higher magnification of cell shown with asterisk in A and C. Top region of cell of interest is enlarged in E to show the two AVs structures indicated by arrows in B. (F and G) Higher magnification of AVs shown by arrows in E.

and Atg7. We used ERGIC-53 to label the ER-Golgi intermediate compartment and found, after COPI depletion, ERGIC-53 labeling was greatly diminished and appeared dispersed (Fig. 3 B). Both the steady-state distribution of ERGIC-53 in control cells, and the dispersal of the ERGIC-53 in COPI-depleted cells was unaffected by co-depletion of Atg5 or Atg7 (Fig. 3, C and D). These results demonstrate that the increase in GFP-LC3-II and GFP-LC3 puncta after COPI depletion requires the autophagy proteins Atg5 and 7, and show that loss of Atg7 does not affect ERCIG-53 distribution in normal cells, or its redistribution and dispersion after siRNA depletion of COPI.

Correlative microscopy demonstrates that the GFP-LC3–positive structures are AVs

Both the accumulation of GFP-LC3-II and GFP-LC3–positive vesicles suggested that β′-, β-, and α-COP–specific siRNA was causing an increase in the number of AVs. Although GFP-LC3–positive puncta are indicative of the presence of AVs, GFP-LC3 can also form large aggregates which resemble AVs at the light microscopic level (Kuma et al., 2007). Although in our previous work with 293/GFP-LC3 cells we did not observe any aggregation of GFP-LC3 into punctate structures under fed or starved conditions (Chan et al., 2007), we used correlative light-electron microscopy (CLEM) to determine if the GFP-LC3 fluorescent structures seen in the COPI-depleted cells by light microscopy corresponded to membrane-bound AVs. As shown in Fig. 4, the GFP-positive vesicles seen by light microscopy (Fig. 4 B) corresponded to morphologically identifiable AVs (Fig. 4, D–G). Many of the AVs had only a single membrane, and were filled with a variety of sequestered membrane-bound vesicles and electron-dense structures (Fig. 4, F and G and Fig. S3 A). These results confirmed that COPI depletion in 293/GFP-LC3 cells resulted in a significant increase in the number of AVs.

Loss of COPI causes the accumulation of p62- and Ub-containing aggregates

p62/SQSTM1 can associate with LC3 on the membrane of AVs and is sequestered into AVs (Pankiv et al., 2007). Levels and subcellular distribution of p62 are used to monitor autophagic flux; a low or unchanged level of p62 indicates a normal autophagic response and flux, whereas an increased level of p62 indicates a block in the flux, resulting from an inhibition of the pathway and an accumulation of AVs (Klionsky et al., 2008). We therefore decided to ask if distribution of p62 was affected by siRNA depletion of COPI (Fig. 5 A). In control siRNA-treated cells, p62 exhibited a diffuse and cytoplasmic pattern similar to the cytosolic GFP-LC3. However, after siRNA depletion of COPI subunits, the signal for p62 increased and it was found in discrete punctate structures, the majority of which were GFP-LC3 positive (Fig. 5 A). p62 has also been shown to associate with dense protein aggregates (Pankiv et al., 2007); however, using TEM we did not observe these structures in our 293/GFP-LC3 cells.

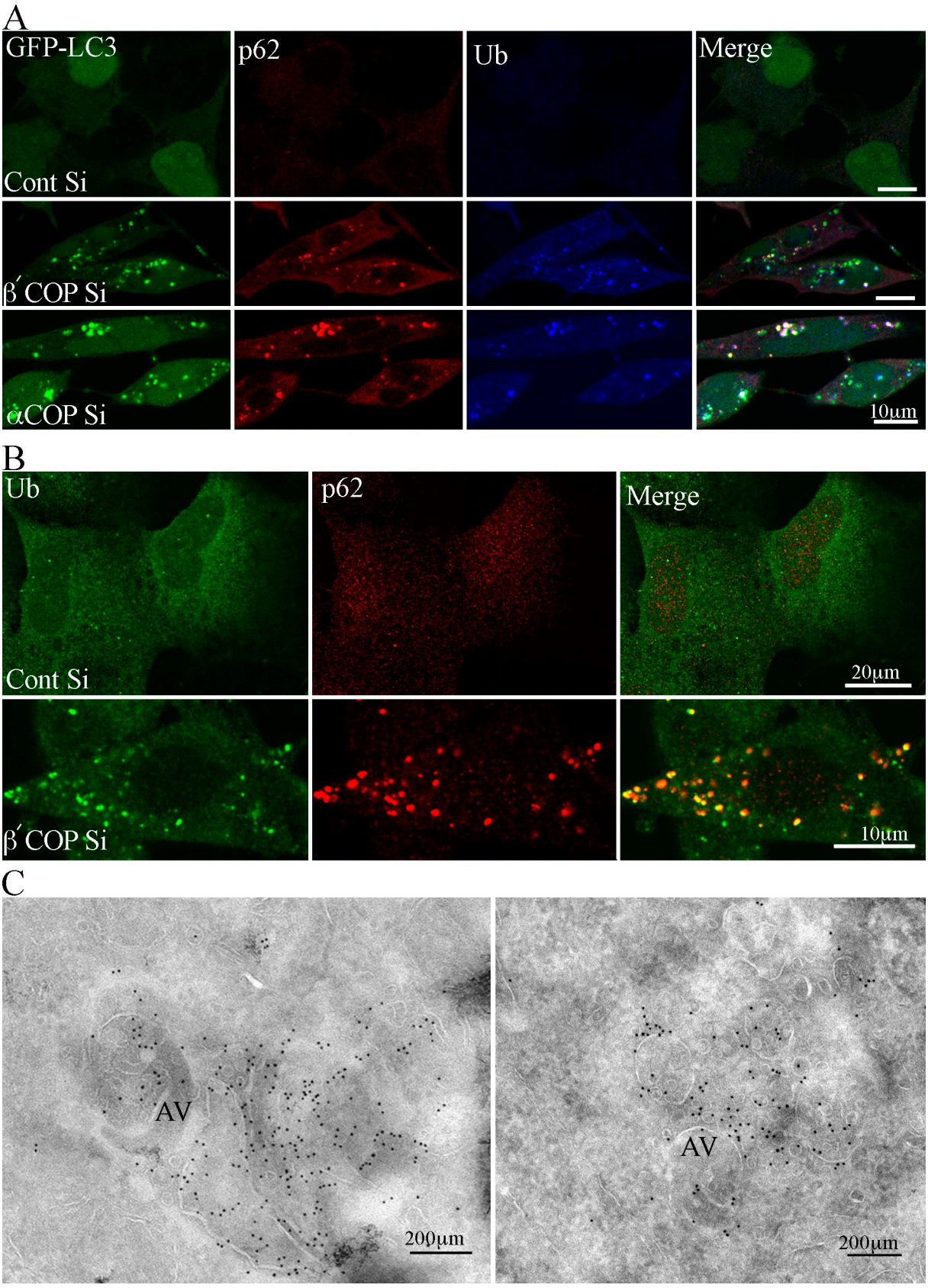

Figure 5. **Ub and p62 accumulate in α- and β′-COP–depleted 293/GFP-LC3 cells.** (A) 293/GFP-LC3 cells were treated with control or β′-COP siRNA for 48 h, then fixed and labeled with anti-p62 and anti-ubiquitin antibodies for colocalization with GFP-LC3. (B) HEK293 cells treated as in A and labeled with anti-ubiquitin and anti-p62 antibodies. (C) Cryosections from β′-COP–depleted cells were labeled with anti-Ub antibodies followed by 10-nm protein A–gold. AV, autophagosomes.

p62 has been shown to bind ubiquitinated proteins via a conserved UBA motif (Pankiv et al., 2007), so we next examined the distribution of ubiquitin (Ub) after siRNA knockdown of COPI. Interestingly, after siRNA depletion of COPI we found Ub distribution was altered, and behaved similarly to p62. Ub had a diffuse appearance in control siRNA-treated cells, and a punctate distribution after siRNA-mediated COP depletion. In addition, a large number of the Ub-positive punctate structures were also positive for GFP-LC3 (Fig. 5 A). Using HEK293A parental cells we also observed after depletion of β′-COP that p62 and Ub redistributed into punctate structures, which were largely colocalized (Fig. 5 B).

Next we performed cryo-immuno EM to gain an understanding of the morphology of the GFP-LC3–positive structures that contained p62 and Ub. Unfortunately, we were unable to label the p62 using commercially available antibodies, but we could detect Ub in cryosections. After siRNA-mediated depletion of β′-COP we observed two major populations of Ub-positive membranes: one population were AVs on which ubiquitin was detected on the limiting cytosolic surface membrane as well as on internal membranes, and the second consisted of small vesicles (less than 100 nm), the outer surface of which was decorated with Ub (Fig. 5 C and Fig. S4). In β′-COP–depleted cells the morphology of the Ub-labeled structures was very similar to that seen after labeling with GFP to detect the GFP-LC3 cells (Fig. S4). Numerous small vesicles, tubules, and AVs, which resembled immature autophagosomes (AVis), were found to be decorated with Ub and GFP-LC3 on their cytoplasmic surface, and well as on internal membranes. These results suggest that after COPI depletion ubiquitinated proteins, and most likely p62, were present on the membrane of small vesicles and tubules, as well as on the cytoplasmic surface of AVs, and on internal membranes within the AVs.

AVs induced by COPI depletion are not acidic or degradative

The large numbers of GFP-LC3 AVs in COPI-depleted cells suggested that either the rate of AV formation was significantly increased, or that AV maturation and consumption was inhibited. An increased autophagic rate should result in an increased degradative capacity of the cells, whereas if autophagosome consumption or maturation is inhibited, degradation of autophagic substrates should be reduced. To assay for the degradative capacity of AVs in the COPI-depleted cells we measured long-lived protein degradation as an indicator of autophagic activity (Fig. 6 A). In siControl unstarved cells, long-lived protein degradation occurred at a low basal level, and increased after a 2-h starvation, as expected. However, after β′-COP depletion, despite the large increase in GFP-LC3-II and GFP-LC3–positive AVs in unstarved cells, there was no change in basal levels of protein degradation (Fig. 6 A). This result suggests an impairment in the degradative capacity of the AVs formed in COP-depleted cells. However, the siRNA COPI-depleted cells were still able to respond to starvation-induced autophagy as protein degradation could be increased after 2 h starvation.

AVi/d and autolysosomes are known to be acidic compartments. To understand more about the properties of the AVs in COPI-depleted cells, in particular why they are not degradative, we next asked if the GFP-LC3–positive AVs were acidic using Lysotracker red (LTR), which accumulates in acidic compartments. In previous studies it was shown that after 2-h amino acid starvation ∼40% of AVs are LTR positive, and contain endosomal markers (Bampton et al., 2005). Using β′- and α-COP–depleted cells incubated in growth medium, we found that the majority of the GFP-LC3–positive structures did not accumulate LTR (Fig. 6 B). Similar results were obtained using DAMP staining, which also accumulates in acidic compartments (not depicted). To further confirm that the lack of GFP-LC3 and LTR colocalization was not due to quenching of the GFP-tag in acidic compartments (which would mask the presence of accumulating GFP-LC3), we looked at total LC3 accumulation using anti-LC3 antibodies in COPI-depleted 293/GFP-LC3 cells. LC3 immunoreactivity should not be sensitive to lumenal acidity. We found a complete overlap of the two signals in COPI-depleted cells, in contrast to siControl starved cells, which showed two immunoreactive populations of LC3, one which overlapped with GFP-LC3, while the other did not (Fig. S3 B). These results confirm that after COPI depletion we can detect all the GFP-LC3–positive AVs using the GFP-tag, and that these AVs were not degradative or acidic.

Dunn (1990) postulated that AVs become acidified before lysosomal enzymes are delivered by fusion with endocytotic compartments, and this may occur by sequential fusion with different types of endosomes; the first to fuse would be endosomes containing the vacuolar (V) proton-ATPase (V-ATPase), but without lysosomal enzymes. To understand if the lack of degradative capacity in the accumulating AVs was only a consequence of the defect in acidification, or if lysosomal enzyme targeting was also affected by loss of COPI, we asked if the COPI-depleted cells had active lysosomal enzymes by examining the levels of Magic Red RR_2, a fluorogenic substrate which detects active cathepsin B (Fig. 6 C). By FACS analysis, there was no difference in the level of cathepsin B between starved control cells and siCOPI-depleted cells. In addition, we confirmed that the COPI-depleted cells contained active cathepsin D by immunoblotting cell lysates; in both control cells and siRNA-treated cells depleted of β′-, β-, and α-COP, and Rab1a/b, we detected similar levels of the 31-kD mature cathepsin D heavy chain (Fig. S5 A).

Our data support the conclusion that the accumulation of GFP-LC3 AVs in COPI-depleted cells is not a consequence of an indirect effect on the entire endosomal–lysosomal pathway as the COPI-depleted cells still have a degradative capacity and normal levels of lysosomal enzymes.

GFP-LC3 autophagosomes are LAMP1 and 2 positive

Lysosomal-associated membrane protein1 and 2 (LAMP1 and 2) are found on late endosomes and lysosomes, and have also been shown to be essential for the maturation of AVs (Saftig et al., 2008). Therefore, we asked if after COPI depletion, the distribution of LAMP1 and 2 in endosomal membranes was altered, and if they were present on GFP-LC3–positive AVs. After COPI depletion the overall distribution of LAMP1 and 2 was not significantly changed. However, many of the GFP-LC3–positive AVs contained LAMP1 (not depicted) and LAMP2

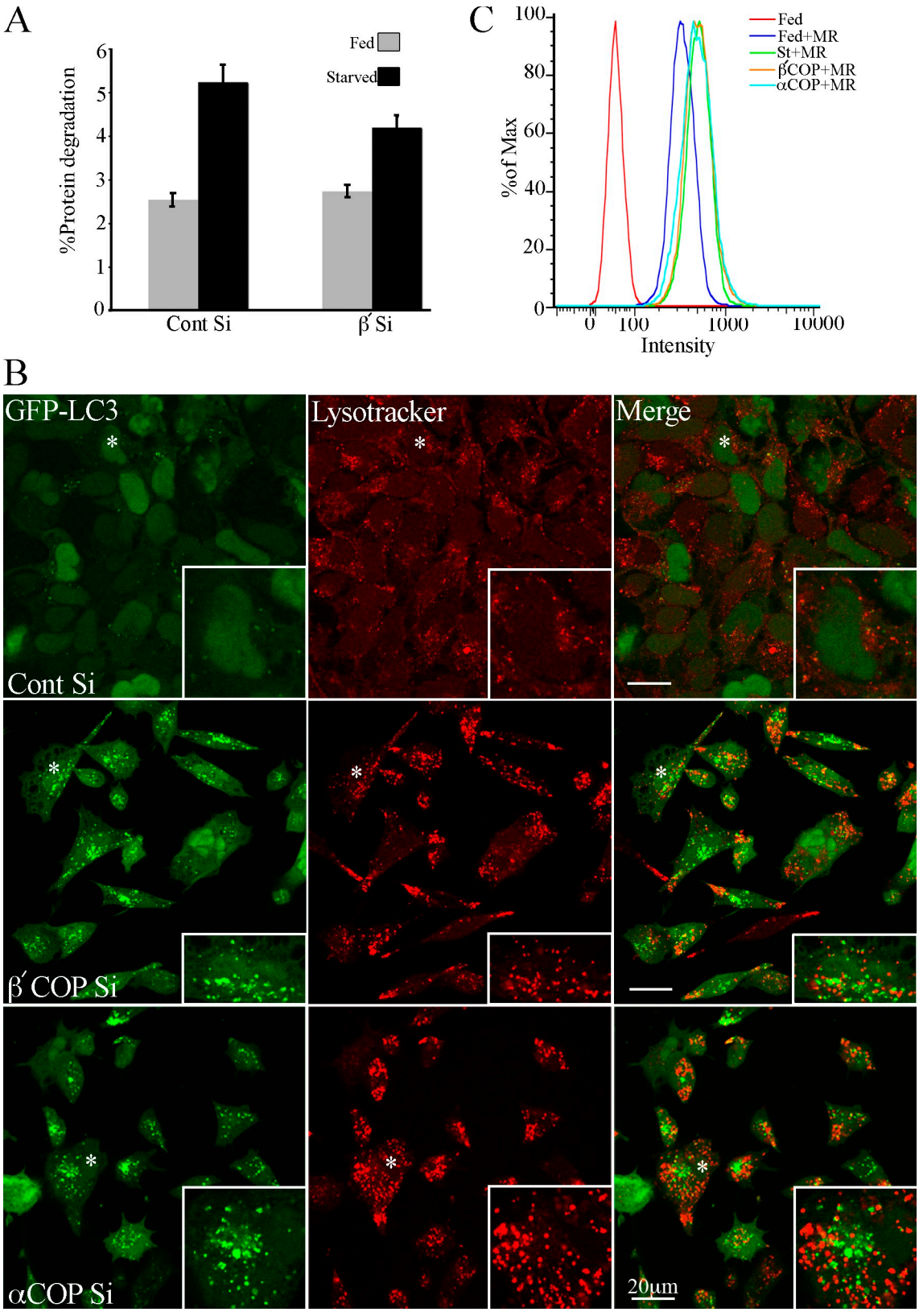

Figure 6. **AVs in COPI-depleted cells are not degradative.** (A) Long-lived protein degradation was assessed 72 h after transfection with control or β′-COP siRNA in 293/GFP-LC3 cells. Cells were either starved of amino acids for 2 h (St) or incubated in fresh growth medium (Fed) for 2 h. The amount of protein degradation is presented as mean ± SEM. (B) siControl-treated cells and β′- and α-COP were depleted for 48 h, then incubated with Lysotracker red (50 nM) for 30 min before fixation. Merged image shows very little colocalization of GFP-LC3 AV-positive structures. Asterisk shows cell enlarged in inset. (C) After β′- and α-COP siRNA depletion, Magic Red-RR_2 (MR) was used to detect active cathepsin B in cells which were fed or starved (St) for 2 h. The intensity of MR labeling was measured in live cells by flow cytometry.

(Fig. 7 A). We next used EM to examine the maturation stage of the AVs which were GFP-LC3– and LAMP2-positive. We labeled cryosections from β′-COP–depleted cells with anti-LAMP2 antibodies and anti-GFP to detect GFP-LC3 (Fig. 7 B). GFP-LC3 was detected on the outer AV membranes as well as on internal membranes and adjacent vesicles. In double-labeled sections, LAMP2 had a similar distribution to GFP-LC3. The AVs labeled by LAMP2 and GFP contained internal membranes, and resembled the AVs labeled by anti-Ub (see Fig. 5 and Fig. S4). However, although the presence of LAMP2 on the GFP-LC3–positive AVs suggests they have undergone fusion with either late endosomes, or lysosomes, we could not detect many AVds by TEM in the siRNA COPI-depleted cells.

Early endosomal markers and TGN46 are found in GFP-LC3–positive AVs

One hypothesis was that AVs formed after siRNA-mediated COPI depletion were acquiring LAMP2 by fusion with late endosomes. As an alternative hypothesis, LAMP2 could also be delivered to AVs by vesicular trafficking from the TGN in vesicles that do not contain MPR (Chapuy et al., 2008) or from early endocytotic compartments such as vesicular endosomes (VEs). Small VEs and MVBs, identified by internalized electron-dense tracers after 10 min incubation, have been shown to fuse preferentially to AVis: About 45% of these endocytotic VEs and MVBs label for Lgp120 (LAMP2), but none label with cathepsin D (Liou et al., 1997). We therefore examined the distribution of TGN46 and the CI-MPR, which cycle between the Golgi/trans-Golgi network (TGN) and plasma membrane via endosomal compartments. Surprisingly, TGN46 and CI-MPR behaved differently after COPI depletion: TGN46 relocalized to punctate structures, while the juxtanuclear accumulation of CI-MPR observed in control cells was lost (Fig. 8 A and Fig. S5 B). The punctate TGN46 structures colocalized with GFP-LC3 (Fig. 8 A), suggesting that the trafficking routes through which TGN46 is sorted may converge with the AVs formed after COPI depletion.

As TGN46 has been recently shown to exit from early endosomes, whereas MPR is thought to exit from late endosomes (Ganley et al., 2008), we asked if markers for early or late endosomes were found in the GFP-LC3 AVs after COPI depletion. We examined markers for early endosomes (early endosomal autoantigen 1 [EEA1]) and late endosomes and MVBs (lysobisphosphatidic acid [LBPA]). No colocalization of GFP-LC3 was seen with LBPA (unpublished data), but we found a small fraction of GFP-LC3–positive, EEA1-positive Avs; however, more frequently GFP-LC3 was juxtaposed to EEA1 (Fig. 8 B). We examined siControl cells after starvation and found a very low colocalization of GFP-LC3 and EEA1 (Fig. 8 B). However, a population of endogenous LC3 was colocalized with, and found on adjacent EEA1-positive early endosomes (Fig. 8 C). We conclude that AVs can fuse with EEA1-positive early endosomes, and that in control cells the absence of colocalization of GFP-LC3 with EEA1 is due to a quenching of GFP in EEA1-positive structures. Furthermore, after COPI depletion the GFP-LC3–positive structures appear docked to EEA1-positive early endosomes.

To further explore the effect of COPI depletion, we followed the internalization of a fluid phase marker, rhodamine-labeled dextran. In the siRNA COPI-depleted cells, many GFP-LC3–positive AVs contained Rho-dextran (Fig. 8 D), supporting the hypothesis that the endocytic vesicles can fuse with AVs. The fact that the GFP-LC3–positive AVs do not have a substantial overlap with EEA1 suggests that loss of COPI inhibits fusion of the AVs with EEA1-positive endosomes, and that inhibition of this fusion step prevents maturation of the AVs.

Endosomal trafficking is disrupted after COPI depletion

To further understand the maturation defect which results in an accumulation of Avs we examined the function of the early endocytic pathway after siRNA depletion of COPI. Previous reports have demonstrated a role of COPI in endosomal transport, endosome maturation, and MVB formation (Whitney et al., 1995; Guo et al., 1996; Daro et al., 1997; Styers et al., 2008). These previous reports showed that transferrin (Tfn) uptake was altered, but did not address EGF internalization and degradation quantitatively. Recently, it has been suggested that these two endocytosed molecules could undergo a differential interaction and sorting with EEA1-positive endosomes (Leonard et al., 2008). Therefore, we examined these two pathways to define the defect in early endosomal trafficking after COPI depletion, which resulted in an inhibition of autophagy.

To measure the function of the early endosome/recycling endosome we examined Tfn uptake, using Alexa 555–labeled Tfn in 293/GFP-LC3 cells. After 48 h β′-COP depletion, a short 2-min and longer 30-min incubation with Tfn revealed a surface accumulation of Tfn, and a reduction in the amount internalized compared with control siRNA-treated cells (Fig. 9, A and B). Longer incubations revealed a delayed recycling in COPI-depleted cells, whereas the majority of Tfn was recycled in control cells, and a colocalization of Tfn with GFP-LC3–positive AVs (Fig. 9, B and C). This result is supported by data showing an inhibition of Tfn internalization after δ- and β-COP depletion in an siRNA screen for regulators of Tfn uptake (Galvez et al., 2007), and after depletion of β-COP (Styers et al., 2008).

Next we examined EGFR trafficking to monitor uptake and transport into late endosomes, using ^{125}I-EGF as a quantitative measure of endosomal function in HeLa cells after COPI depletion. HeLa cells were used for this experiment because 293/GFP-LC3 cells detached during the acidic wash. After β′-COP depletion, HeLa cells were serum starved and then stimulated with the ^{125}I-EGF for 10 min at 37°C, and then the cells were chased for 30, 60, 120, and 180 min (including the 10-min stimulation). The amount of ^{125}I-EGF internalized after 10 min incubation was reduced by ∼30% (Fig. 9 D) in β′-COP–depleted cells compared with control siRNA cells. Over a 3-h chase in β′-COP–depleted cells, ∼50% less ^{125}I-EGF was degraded compared with the control cells (Fig. 9 E). Our results with Alexa 488–Tfn and ^{125}I-EGF show that both the Tfn and EGF pathways are affected by COPI depletion: early endosome function is impaired leading to reduced internalization from the plasma membrane, reduced recycling from perinuclear early endosomes, and reduced degradation in late endosomes.

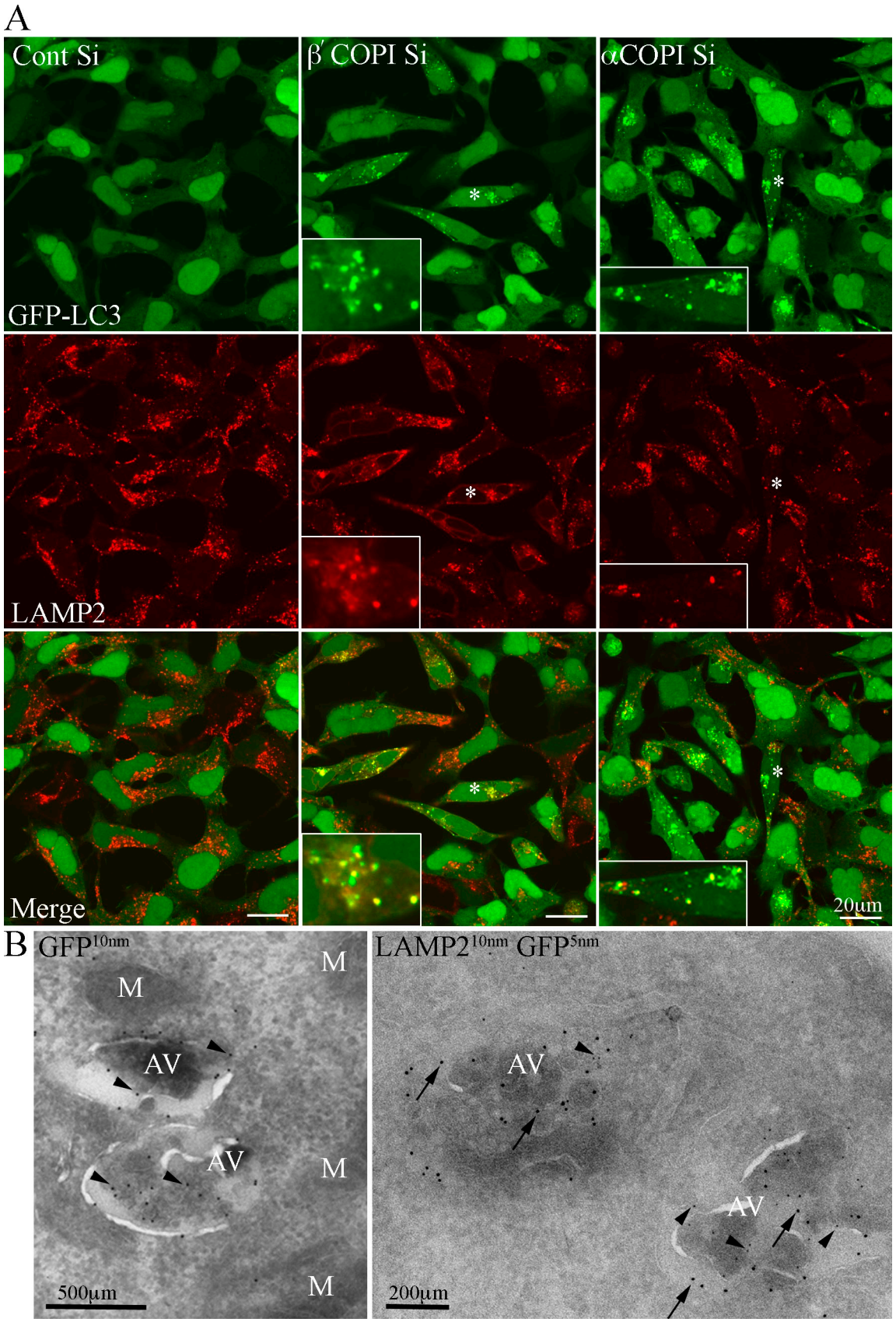

Figure 7. **GFP-LC3 AVs are LAMP2 positive.** (A) 293/GFP-LC3 cells were incubated with control or β′- or α-COP siRNA for 48 h, fixed and labeled with anti-LAMP2 antibodies, followed by Alexa 555 anti–mouse antibodies. After COPI depletion many GFP-LC3–positive AVs are positive for LAMP2. Asterisk indicates cell enlarged in inset. (B) Cryosections of β′-COP-depleted cells labeled with anti-GFP (left) or anti-GFP and anti-LAMP2 (right) followed by protein A–gold as indicated. AV, autophagosomes, M, mitochondria.

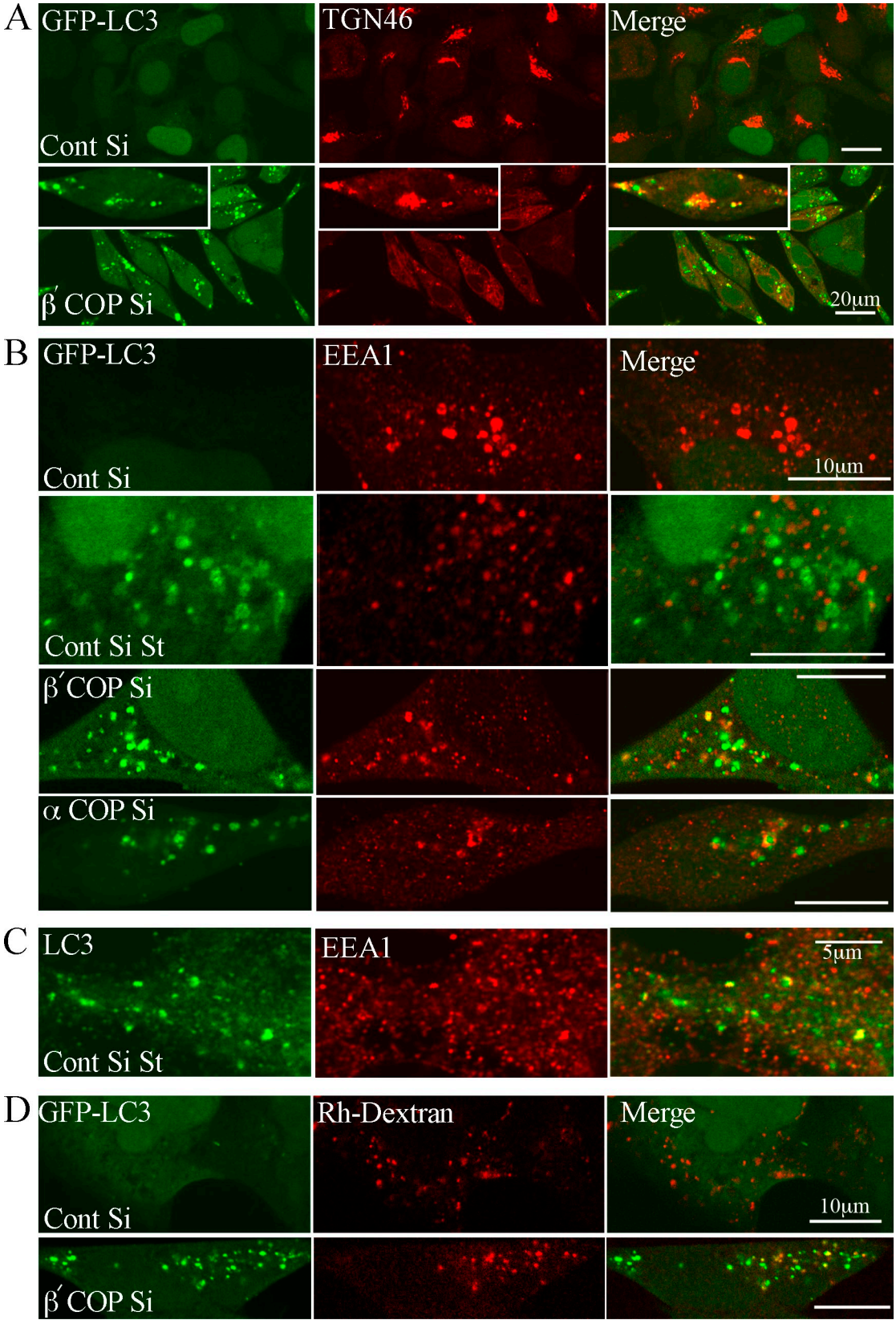

Figure 8. **GFP-LC3–positive AVs colocalize TGN46 and early endocytotic markers after COPI depletion.** (A) 293/GFP-LC3 cells were incubated with siRNA for β′-COP or control siRNA (Cont) for 48 h, processed for immunofluorescence, and labeled with antibodies for TGN46. In (B) siRNA-treated cells were fixed and labeled, or starved for 2 h (St), and labeled with antibodies to EEA1. (C) Control-starved HEK293 cells were labeled for endogenous LC3 and EEA1 by double labeling after methanol fixation. (D) After siRNA treatment, rhodamine-labeled dextran was internalized for 20 min, followed by a 40-min chase after which the 293/GFP-LC3 cells were fixed and analyzed by confocal microscopy.

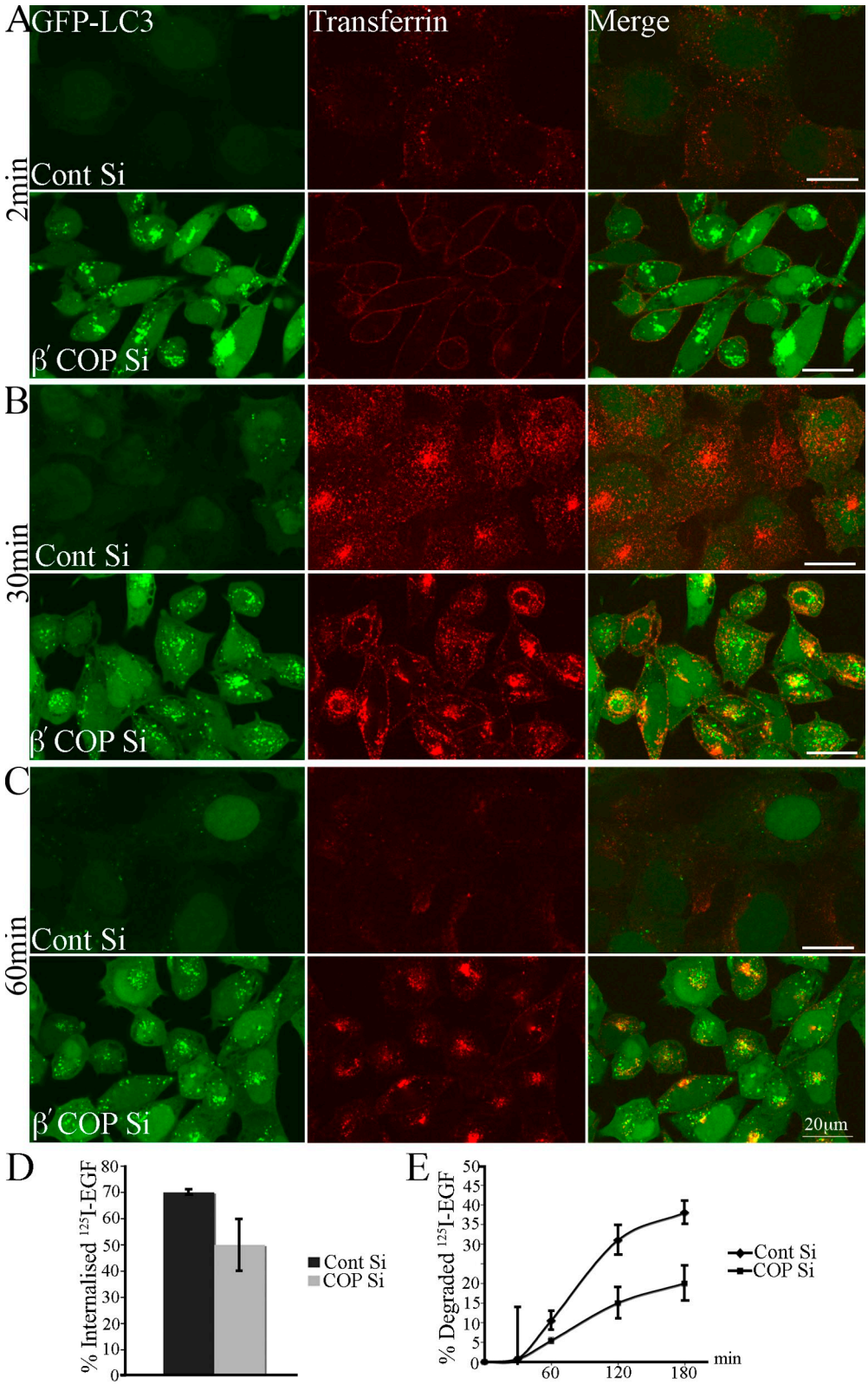

Figure 9. **Transferrin and EGF trafficking is inhibited by COPI depletion.** 293/GFP-LC3 cells were treated with β′-COP siRNA or control siRNA. After 48 h cells were incubated with Alexa 555 transferrin (A) for 2 min, (B) 30 min, or (C) 30 min followed by a 30-min chase, then washed and fixed and analyzed by confocal microscopy. (D and E) ^{125}I-EGF was added to HeLa cells after 48 h of siRNA depletion of β′-COP, or control siRNA for 10 min. The cells were then washed as described in the Materials and methods, and chased for 30, 60, 120, and 180 min (including 10-min incubation). (D) The amount of ^{125}I-EGF internalized was shown as a percentage of the total ^{125}I-EGF taken up in 10 min. (E) The amount of degraded ^{125}I-EGF was determined as a percentage of the total radioactivity present after TCA precipitation over the total ^{125}I-EGF internalized. The experiment was performed three times in duplicate and the data shown is the mean ± SEM. The significance was determined by Student's *t* test. *, $P \leq 0.05$.

A consequence of altered trafficking of growth factor receptors could be a decrease in the uptake of nutrients and the generation of a starvation signal. Thus, COPI depletion could potentially be causing a chronic starvation signal by down-regulating Tfn and EGF receptors. To investigate this possibility we took three approaches. First, we mimicked growth factor receptor deprivation by withdrawing serum from the cells. Although we did observe an induction of GFP-LC3–positive AVs, the kinetics of formation and consumption was different from the effects of COPI depletion; a maximum response was obtained at 15 h serum starvation, which disappeared after 24 h serum starvation. Second, we measured amino acid uptake in COPI-depleted cells in comparison to siRNA treated control cells in full medium or after starvation. In control starved cells we observed a 10-fold increase in [^{14}C]-valine uptake, but basal uptake in the COPI-depleted cells. In fact, after 72 h COPI depletion, the levels of valine uptake per cell were identical to control fed cells. Interestingly, COPI-depleted cells after 2 h starvation showed a similar increase to control starved cells. Our third approach was to use 11 mM methyl pyruvate (Guenther et al., 2008), shown to function as a transporter-independent source of nutrients; addition of methyl pyruvate 24 h before harvesting COPI-depleted cells had little effect on GFP-LC3-II accumulation, whereas its addition inhibited the GFP-LC3-II conversion in control starved cells (unpublished data).

Discussion

Nascent AVs (AVis) are double-membrane vesicles containing sequestered cytoplasmic proteins and organelles. AVis only become degradative (AVds) when they fuse with endosomes. It has been proposed that a sequential fusion event between AVis and different types of endosomal vesicles or endosomes is required for AVi maturation to AVds or autolysosomes (Dunn, 1990; Eskelinen, 2005). Although recent data have highlighted the importance of late endocytic machinery in the autophagic response, in particular the ESCRT complex (Filimonenko et al., 2007; Lee et al., 2007; Rusten et al., 2007), there is no direct evidence that fusion of early endosomes is required for AV maturation. Through our analysis of β′-COP, identified as a potential negative regulator of autophagy (Chan et al., 2007), we have shown that functional early endosomes are required for autophagy.

We show that loss of COPI subunits β′, α, and β results in an inhibition of AV maturation and subsequently causes an accumulation of AVs. The accumulation of AVs after COPI depletion is robust, and raises the question of whether basal autophagy is also increased by loss of COPI. This hypothesis is difficult to directly test in our model system, as the siRNA depletion of COPI occurs over 48 h and the levels of COP subunits decrease gradually. However, we have determined the extent of AV accumulation that could be detected in control, untreated 293/GFP-LC3 cells after basal autophagy was blocked for 5, 25, or 50 h by culturing the 293/GFP-LC3 cells in normal culture medium in the presence of leupeptin (unpublished data). After 25 h of leupeptin treatment there was a significant accumulation of basal AVs, which was comparable to 48 h siRNA depletion of COP subunits, leading us to suggest that the primary effect exerted by COPI depletion was an inhibition of maturation of AVs that formed in basal conditions.

The COPI complex has been shown to function in both anterograde and retrograde transport to and through the Golgi complex, as well as in early endosome maturation. We found that loss of either β′-, α-, and β-COP, gave identical results on both Golgi morphology and AV accumulation. Previous data using a stable temperature sensitive CHO cell line (ldl-F cells), in which ε-COP is degraded at the nonpermissive temperature, show a loss of the Golgi complex similar to our observations (Guo et al., 1994), whereas siRNA depletion of β-COP (Styers et al., 2008) showed a collapse of ERGIC and Golgi markers into a common compartment. The differences in Golgi morphology between our β-COP depletion experiments and those in Styers et al. [2008] are likely to be caused by differences in the level of β-COP depletion, or differences in the levels of the other COPs: we reproducibly saw α-COP decreased after β′- and β-COP depletion, and β′-COP decreased after β-COP depletion.

Having observed a profound affect on the Golgi complex after 48 h of β′-COP depletion, we asked if the disruption of the Golgi complex was responsible for the accumulation of AVs. In a time-course experiment we observed that after 24 h siRNA depletion Golgi morphology was already perturbed, suggesting that Golgi fragmentation was the cause of the increase in AVs. We tested this hypothesis using siRNA depletion of Rab1, which has a similar effect of Golgi morphology and function (Haas et al., 2007), and saw that disassembly of the Golgi, by itself, did not cause an accumulation of AVs.

We found an increased number of p62 and Ub-positive structures, which colocalize with GFP-LC3 after COPI depletion, in agreement with previous data demonstrating an increase in p62 levels after a block in autophagic turnover (Pankiv et al., 2007). Furthermore, as p62 has an ubiquitin-associated domain (UBA), which interacts with Ub (Geetha and Wooten, 2002), the colocalization we detect of Ub with p62 and GFP-LC3 in AVs represents a pool of Ub sequestered into AVs via an interaction with p62. Intriguingly, our data also show that some of the Ub is present on the cytoplasmic surface of small vesicles and tubules, and these are also sequestered into AVs. The origin of these small vesicles and tubules is unknown, but we speculate that they originate from compartments that, after COPI depletion, have undergone vesiculation or other alterations leading to damage and recruitment of Ub. Although we have no data to support this hypothesis, and indeed we did not detect a colocalization of GM130 with Ub, we speculate that ubiquitination of the fragmented or damaged compartments may be a signal to target them to AVs. It is also possible that ubiquitinated vesicles or compartments accumulated in regions where AVs are forming or expanding and were nonselectively sequestered. Further experiments are required to determine the origin and fate of the ubiquitinated vesicular structures.

After siRNA depletion of COPI subunits we observed an inhibition of Tfn internalization and recycling, in agreement with previous reports (Guo et al., 1994; Daro et al., 1997; Styers et al., 2008). In addition, we found β′-COP depletion caused a decreased internalization and degradation of ^{125}I-EGF, in line with previous results showing a delayed delivery of Texas red–labeled biotinylated EGF to lgp-95 (lysosomal glycoprotein-95) positive structures (Daro et al., 1997). Endosomes have been shown to have COPI coats and the early studies demonstrated a

role for COPI in endocytosis of virus (Whitney et al., 1995), in endosomal carrier vesicle formation and MVB maturation using the inhibitory M3A5 monoclonal raised against β-COP (Whitney et al., 1995; Aniento et al., 1996) and in assays using the ldlF cells (Gu et al., 1997). More recently, in yeast COPI has been shown to be required for endosomal transport to the vacuole, similar to the class E yeast vacuolar protein sorting (Vps) mutants involved in MVB formation (Gabriely et al., 2007). Finally, the endosomal pool of COPI has been shown to be used by anthrax lethal factor for translocation across endosomal membranes (Tamayo et al., 2008), providing independent evidence for a role of COPI in endosome function. An alternative scenario that we have tested is that COPI depletion through its inhibition of Tfn and EGF internalization may generate a starvation signal, inducing autophagy independently of endosome function. Although we found serum deprivation induced GFP-LC3 AV formation after a short serum starvation, the cells adapted to the absence of serum by 24 h and GFP-LC3 AVs were no longer detected. In addition, our assays for amino acid uptake and sensitivity to methyl pyruvate suggest that the COPI-depleted cells are not in a state of chronic starvation due to loss of growth factor signaling.

We hypothesize that loss of the endosomal pool of COPI results in the accumulation of GFP-LC3–positive endosomes due to a defect in early endosome maturation. The accumulating AVs are not acidic or LTR positive, and lack lysosomal proteases such as cathepsin D (unpublished data), but are LAMP positive and contain TGN46.

Our data demonstrating a colocalization of endogenous LC3 with EEA1 provide strong evidence that under normal starvation conditions there is fusion of early endosomes with AVs, and suggest that the EEA1-positive endosomes are involved in AV maturation. Other evidence in hepatocytes and exocrine pancreatic cells supports the notion that early endosomes can fuse with AVis (Gordon and Seglen, 1988; Tooze et al., 1990). In contrast, and in agreement with Fass et al., 2006 we did not see a robust colocalization of GFP-LC3 with EEA1. We attribute this difference to quenching of GFP in the EEA1-positive compartment. However, we have tested the requirement for EEA1 in AV maturation by transfection of an siRNA shown previously to deplete EEA1 (Leonard et al., 2008), and found that loss of EEA1 did not result in the accumulation of GFP-LC3–positive AVs, or GFP-LC3-II (unpublished data). Why does loss of EEA1 not lead to AV accumulation as seen with COPI disruption?

Recent data examining the role of EEA1 in endocytosis suggest that EEA1-positive endosomes may have a specialized function for sorting EGFR into a degradative compartment, and may not be required for Tfn recycling (Leonard et al., 2008). It was proposed that Tfn-containing endosomes only associate with EEA1-positive endosomes, while EGF containing endocytic vesicles dock and fuse with the EEA1-positive endosomes due to a requirement for Rab5. We speculate that under basal conditions, AVi maturation can by-pass the EEA1-dependent endosome, although this remains to be further demonstrated. Our data showing the requirement of COPI in both Tfn and EGF trafficking indicate that COPI might have broader functions in endosomal trafficking possibly by acting upstream of the EEA1-positive endosomes. What are these endosomes upstream of EEA1? One possibility is that they are VEs, previously demonstrated to undergo fusion with AVis, and are both LAMP2 positive, and accessible to endocytotic tracers after 10 min (Liou et al., 1997). Further experiments are required to characterize these VEs, and for instance to investigate if they contain TGN46, before we can fully understand the role of this compartment.

Our data demonstrate that GFP-LC3–positive AVs accumulated in COPI-depleted cells due to an inhibition of early endosome function, resulting in the formation of AVs that cannot mature. Previous data have shown that AV accumulation occurs after disruption of ESCRT on late endosomes (Filimonenko et al., 2007; Kim et al., 2007; Lee et al., 2007). Collectively, these results demonstrate a role for both early endosomes and late endosomes in autophagy. Our data provide direct evidence that early endosome fusion with AVs is a prerequisite for AV maturation, and occurs before fusion with late endosomes and MVBs. Whether the inhibition of early endosome function and consequently AVi maturation gives rise to a pathological disease state similar to the neurodegenerative diseases associated with ESCRT loss of function remains to be determined.

Materials and methods

Cell lines and reagents

HeLa, HEK293A, and 293/GFP-LC3 cells (Chan et al., 2007), a stable HEK293A cell line expressing rat GFP-LC3, were cultured in DMEM containing 10% FCS. For indirect immunofluorescence and EM, HEK293 or 293/GFP-LC3 cells were plated on poly-D-lysine–coated coverslips. Salubrinal was from Axxora; Radionucleotides were from PerkinElmer; Oligofectamine 2000 was from Invitrogen; Tunicamycin was from Sigma-Aldrich.

Transfection and siRNA reagents

siRNAs were transfected with Oligofectamine using the manufacturer's protocol. All siRNAs were purchased from Thermo Fisher Scientific and the sequences are as follows: Control nontargeting siRNA duplex (D-001210-021), β′-COP (D-019847-01), β-COP (D-017940-01), and α-COP (M-011835-01). Rab1a and 1b (L-008283-00 and L-008958-01), sec23A and sec23B (M-009582-00 and M-009592-00), Atg5 (M-004374-01), and Atg7 (M-020112-01). EEA1 siRNA was as published (Leonard et al., 2008). Cells were transfected with siRNA for 48–72 h unless otherwise stated.

Immunoblotting

Immunoblotting was performed on cells lysed in 1x SDS sample buffer. Antibodies used were rabbit anti-β′-COP (891) and rabbit anti-α-, -β′-, -γ-COP (883), both from Prof. Felix Wieland (University of Heidelberg, Heidelberg, Germany), and rabbit anti-EAGE β-COP (STO235) (Duden et al., 1991). Rabbit anti-Atg5 (Cosmo Bio Ltd); anti-Atg7 (Novus); rabbit anti-Rab1 (Santa Cruz Biotechnology, Inc.); mouse anti-Sec23 (ABR); rabbit anti-GFP [Dr. T. Hunt (CRUK)]; monoclonal anti-LC3 (5F10) (Nanotools); rabbit anti-calreticulin (Bioquote); goat anti-cathepsin D antibody (Santa Cruz Biotechnology, Inc.); rabbit anti-tubulin (Abcam). HRP-conjugated secondary antibodies were revealed using ECL (GE Healthcare) according to the manufacturer's instructions.

Indirect immunofluorescence

Indirect immunofluorescence was performed using a standard protocol on cells fixed with 3% PFA in PBS, permeabilized in 0.2% Triton X-100, and a 20-min incubation in 0.5% BSA. For endogenous LC3 (using 5F10) we fixed the cells with −20°C methanol for 5 min. Cells were then incubated with primary antibody followed by a secondary antibody in PBS containing 0.1% BSA. Mouse LAMP2 (CD107B) antibody was from BD Biosciences, guinea pig anti-p62 from Progen, mouse anti-CI-MPR from Abcam, rabbit anti-ubiquitin from Dako, mouse anti-ERGIC-53 from Qbiogene, mouse anti-GM130 from BD Biosciences, and sheep anti-TGN46 from AbD Serotec. Rabbit anti-EEA1 antibody was a gift of M. Clague (University of Liverpool, UK). Alexa-conjugated transferrin, secondary antibodies, and Lysotracker red were from Invitrogen. Lysotracker was used following the manufacturer's instructions. Rhodamine-labeled dextran (Invitrogen)

was used at 0.5 mg/ml in growth medium. Cells were examined and imaged with a Zeiss LSM 510 laser-scanning confocal microscope equipped with a 63x, 1.4 NA, Plan Apochromat oil-immersion objective (Carl Zeiss, Inc.). Images were processed using LSM 510 software. Magic Red-$(RR)_2$ (Immunochemistry Technologies, LLC) was added to the adherent cells for 20 min, after which they were removed by trypsinization, and analyzed in a LSR II FACS (Becton Dickinson) using excitation of 592 nm and emission of 628 nm.

Long-lived protein degradation and amino acid uptake

Long-lived protein degradation was performed as described previously (Chan et al., 2007). In brief, 293/GFP-LC3 cells were transfected with siRNA against β′-COP. 48 h later, labeling medium (DMEM, 10% dialyzed FBS containing [^{14}C]-valine [0.2 μCi/ml, GE], and 65 μM unlabeled valine) was added to the cells. After 18 h, the labeling medium was replaced with chase medium (DMEM, 10% FCS, and 2 mM unlabeled valine) for 4 h. After the chase, cells were incubated in EBSS and 2 mM valine for 2 h to stimulate autophagy. The cells and media were collected, and separately subjected to trichloroacetic acid (TCA) precipitation by the addition of ice-cold TCA to 10%. The percentage of autophagic degradation was quantified as (TCA-soluble counts from medium)/(TCA-soluble counts from medium) + (TCA-insoluble counts from the cells) (Gronostajski and Pardee, 1984).

Amino acid uptake was performed using 0.2 μCi/ml [^{14}C]-valine in labeling medium for 3 h either to control cells, or cells after 72 h siRNA transfection. Radioactivity was measured in the cells after washing. Viable cell number was determined from duplicate wells.

EGF internalization and degradation

HeLa cells were transfected with siRNA using Oligofectamine, and 72 h later cells were serum starved for at least 1 h followed by an incubation with ^{125}I-EGF (1 ng/ml) in binding medium (0.05% BSA in serum-free DMEM) for 10 min at 37°C. Cells were surface stripped using 0.1 M glycine and 0.9% NaCl, pH 3.0, at 4°C, washed with binding medium, and placed in fresh prewarmed 37°C binding medium. After each time point the medium was collected and replaced by fresh medium for the subsequent time point. The collected media were TCA (20% final) precipitated at 4°C for 1 h. TCA-insoluble proteins were pelleted by centrifugation at 14,000 *g* at 4°C, and the soluble supernatant was collected. Cells were lysed in 1% Triton X-100, and the radioactivity in the chase medium, the TCA soluble supernatant, and cell lysates were counted to determine the percentage of EGF degradation and recycling.

Electron microscopy

Cells were fixed in 0.1 M cacodylate containing 2% paraformaldehyde and 2% glutaraldehyde and were then embedded using standard procedures (Hopkins and Trowbridge, 1983). Cryo-immuno-EM was performed on cells fixed with 4% paraformaldehyde/0.1% glutaraldehyde (for ubiquitin and LAMP2 labeling cells were fixed only with PFA) in 0.1 M phosphate buffer, pH 7.4, infused with 2.3 M sucrose and supported in 10% gelatin. Sections (70 nm) were cut at −120°C and picked up in 1:1 sucrose/methylcellulose. Primary antibodies were rabbit anti-ubiquitin (Dako), rabbit anti-GFP antibody (Abcam), and mouse anti-LAMP2 (BD Biosciences). Sections were then labeled using protein A–gold as described previously (Slot and Geuze, 2007). Sections were visualized in a FEI Technai G2 Spirit Biotwin transmission electron microscopic and an Ultrascan 1000 CCD camera and software.

Online supplemental material

Figure S1 shows the effect of β′-, α-, and β-COP on the structure of the Golgi complex by transmission electron microscopy. Figure S2 shows that COPI depletion does not cause ER stress. Figure S3 A shows the morphology of the AVs accumulating in COP-depleted cells by transmission electron microscopy. Figure S3 B confirms GFP-LC3 is not quenched in acidic structures. Figure S4 shows the cryo-immuno electron microscopy of 293/GFP-LC3 cells after 48 h COPI depletion labeled for Ub and GFP. Figure S5 A shows cathepsin D is correctly stored and processed after COPI depletion, or Rab1 depletion. Figure S5 B shows that CI-MPR after COPI depletion is dispersed and not colocalized with GFP-LC3. Online supplemental material is available at http://www.jcb.org/cgi/content/full/jcb.200810098/DC1.

We thank Drs. Giampietro Schiavo and Jöelle Movan for comments on the manuscript, and the Secretory Pathways laboratory, Rose Watson, Hannah Armer, and the London Research Institute EM unit for their help and advice.

We thank Cancer Research UK for support.

Submitted: 15 October 2008
Accepted: 24 March 2009

References

Aniento, F., F. Gu, R.G. Parton, and J. Gruenberg. 1996. An endosomal beta COP is involved in the pH-dependent formation of transport vesicles destined for late endosomes. *J. Cell Biol.* 133:29–41.

Bampton, E.T.W., C.G. Goemans, D. Niranjan, N. Mizushima, and A.M. Tolkovsky. 2005. The dynamics of autophagy visualized in live cells: from autophagosome formation to fusion with endo/lysosomes. *Autophagy.* 1:23–36.

Boyce, M., K.F. Bryant, C. Jousse, K. Long, H.P. Harding, D. Scheuner, R.J. Kaufman, D. Ma, D.M. Coen, D. Ron, and J. Yuan. 2005. A selective inhibitor of eIF2{alpha} dephosphorylation protects cells from ER stress. *Science.* 307:935–939.

Chan, E.Y.W., S. Kir, and S.A. Tooze. 2007. siRNA screening of the kinome identifies ULK1 as a multi-domain modulator of autophagy. *J. Biol. Chem.* 282:25464–25474.

Chapuy, B., R. Tikkanen, C. Muhlhausen, D. Wenzel, K. von Figura, and S. Honing. 2008. AP-1 and AP-3 mediate sorting of melanosomal and lysosomal membrane proteins into distinct post-Golgi trafficking pathways. *Traffic.* 9:1157–1172.

Citterio, C., A. Vichi, G. Pacheco-Rodriguez, A.M. Aponte, J. Moss, and M. Vaughan. 2008. Unfolded protein response and cell death after depletion of brefeldin A-inhibited guanine nucleotide-exchange protein GBF1. *Proc. Natl. Acad. Sci. USA.* 105:2877–2882.

Csukai, M., C.-H. Chen, M.A. De Matteis, and D. Mochly-Rosen. 1997. The coatomer protein beta'-COP, a selective binding protein (RACK) for protein kinase Cepsilon. *J. Biol. Chem.* 272:29200–29206.

Daro, E., D. Sheff, M. Gomez, T. Kreis, and I. Mellman. 1997. Inhibition of endosome function in CHO cells bearing a temperature-sensitive defect in the coatomer (COPI) component epsilon-COP. *J. Cell Biol.* 139:1747–1759.

Duden, R., G. Griffiths, R. Frank, P. Argos, and T.E. Kreis. 1991. β-COP, a 110 kDa protein associated with non-clathrin-coated vesicles and the Golgi complex, shows homology to β-adaptin. *Cell.* 64:649–665.

Dunn, W.A. Jr. 1990. Studies on the mechanisms of autophagy: maturation of the autophagic vacuole. *J. Cell Biol.* 110:1935–1945.

Eskelinen, E.L. 2005. Maturation of autophagic vacuoles in mammalian cells. *Autophagy.* 1:1–10.

Eugster, A., G. Frigerio, M. Dale, and R. Duden. 2000. COP I domains required for coatomer integrity, and novel interactions with ARF and ARF-GAP. *EMBO J.* 19:3905–3917.

Filimonenko, M., S. Stuffers, C. Raiborg, A. Yamamoto, L. Malerod, E.M. Fisher, A. Isaacs, A. Brech, H. Stenmark, and A. Simonsen. 2007. Functional multivesicular bodies are required for autophagic clearance of protein aggregates associated with neurodegenerative disease. *J. Cell Biol.* 179:485–500.

Gabriely, G., R. Kama, and J.E. Gerst. 2007. Involvement of specific COPI subunits in protein sorting from the late endosome to the vacuole in yeast. *Mol. Cell. Biol.* 27:526–540.

Galvez, T., M.N. Teruel, W.D. Heo, J.T. Jones, M.L. Kim, J. Liou, J.W. Myers, and T. Meyer. 2007. siRNA screen of the human signaling proteome identifies the PtdIns(3,4,5)P3-mTOR signaling pathway as a primary regulator of transferrin uptake. *Genome Biol.* 8:R142.

Ganley, I.G., E. Espinosa, and S.R. Pfeffer. 2008. A syntaxin 10-SNARE complex distinguishes two distinct transport routes from endosomes to the trans-Golgi in human cells. *J. Cell Biol.* 180:159–172.

Geetha, T., and M.W. Wooten. 2002. Structure and functional properties of the ubiquitin binding protein p62. *FEBS Lett.* 512:19–24.

Gordon, P.B., and P.O. Seglen. 1988. Prelysosomal convergence of autophagic and endocytic pathways. *Biochem. Biophys. Res. Commun.* 151:40–47.

Gronostajski, R.M., and A.B. Pardee. 1984. Protein degradation in 3T3 cells and tumorigenic transformed 3T3 cells. *J. Cell. Physiol.* 119:127–132.

Gu, F., F. Aniento, R.G. Parton, and J. Gruenberg. 1997. Functional dissection of COP-I subunits in the biogenesis of multivesicular endosomes. *J. Cell Biol.* 139:1183–1195.

Guenther, G.G., E.R. Peralta, K.R. Rosales, S.Y. Wong, L.J. Siskind, and A.L. Edinger. 2008. Ceramide starves cells to death by downregulating nutrient transporter proteins. *Proc. Natl. Acad. Sci. USA.* 105:17402–17407.

Guo, Q., E. Vasile, and M. Krieger. 1994. Disruptions in Golgi structure and membrane traffic in a conditional lethal mammalian cell mutant are corrected by epsilon-COP. *J. Cell Biol.* 125:1213–1224.

Guo, Q., M. Penman, B.L. Trigatti, and M. Krieger. 1996. A single point mutation in epsilon-COP results in temperature-sensitive, lethal defects in membrane transport in a Chinese hamster ovary cell mutant. *J. Biol. Chem.* 271:11191–11196.

Haas, A.K., S. Yoshimura, D.J. Stephens, C. Preisinger, E. Fuchs, and F.A. Barr. 2007. Analysis of GTPase-activating proteins: Rab1 and Rab43 are key

Rabs required to maintain a functional Golgi complex in human cells. *J. Cell Sci.* 120:2997–3010.

Hopkins, C.R., and I.S. Trowbridge. 1983. Internalization and processing of transferrin and the transferrin receptor in human carcinoma A431 cells. *J. Cell Biol.* 97:508–521.

Kim, B.Y., J.A. Olzmann, G.S. Barsh, L.-S. Chin, and L. Li. 2007. Spongiform neurodegeneration-associated E3 ligase mahogunin ubiquitylates TSG101 and regulates endosomal trafficking. *Mol. Biol. Cell.* 18:1129–1142.

Klionsky, D.J. 2007. Autophagy: from phenomenology to molecular understanding in less than a decade. *Nat. Rev. Mol. Cell Biol.* 8:931–937.

Klionsky, D.J., H. Abeliovich, P. Agostinis, D.K. Agrawal, G. Aliev, D.S. Askew, M. Baba, E.H. Baehrecke, B.A. Bahr, A. Ballabio, et al. 2008. Guidelines for the use and interpretation of assays for monitoring autophagy in higher eukaryotes. *Autophagy.* 4:151–175.

Kuma, A., M. Matsui, and N. Mizushima. 2007. LC3, an autophagosome marker, can be incorporated into protein aggregates independent of autophagy: caution in the interpretation of LC3 localization. *Autophagy.* 3:323–328.

Lee, J.A., A. Beigneux, S. Ahmad, S. Young, and F. Gao. 2007. ESCRT-III dysfunction causes autophagosome accumulation and neurodegeneration. *Curr. Biol.* 17:1561–1567.

Lee, M.C.S., E.A. Miller, J. Goldberg, L. Orci, and R. Schekman. 2004. Bidirectional protein transport between the ER and Golgi. *Annu. Rev. Cell Dev. Biol.* 20:87–123.

Leonard, D., A. Hayakawa, D. Lawe, D. Lambright, K.D. Bellve, C. Standley, L.M. Lifshitz, K.E. Fogarty, and S. Corvera. 2008. Sorting of EGF and transferrin at the plasma membrane and by cargo-specific signaling to EEA1-enriched endosomes. *J. Cell Sci.* 121:3445–3458.

Liou, W., H.J. Geuze, M.J.H. Geelen, and J.W. Slot. 1997. The autophagic and endocytic pathways converge at the nascent autophagic vacuoles. *J. Cell Biol.* 136:61–70.

Mizushima, N., B. Levine, A.M. Cuervo, and D.J. Klionsky. 2008. Autophagy fights disease through cellular self-digestion. *Nature.* 451:1069–1075.

Nickel, W., B. Brugger, and F.T. Wieland. 2002. Vesicular transport: the core machinery of COPI recruitment and budding. *J. Cell Sci.* 115:3235–3240.

Nyfeler, B., O. Nufer, T. Matsui, K. Mori, and H.-P. Hauri. 2003. The cargo receptor ERGIC-53 is a target of the unfolded protein response. *Biochem. Biophys. Res. Commun.* 304:599–604.

Ogata, M., S.-i. Hino, A. Saito, K. Morikawa, S. Kondo, S. Kanemoto, T. Murakami, M. Taniguchi, I. Tanii, K. Yoshinaga, et al. 2006. Autophagy is activated for cell survival after endoplasmic reticulum stress. *Mol. Cell. Biol.* 26:9220–9231.

Pankiv, S., T.H. Clausen, T. Lamark, A. Brech, J.-A. Bruun, H. Outzen, A. Overvatn, G. Bjorkoy, and T. Johansen. 2007. p62/SQSTM1 binds directly to Atg8/LC3 to facilitate degradation of ubiquitinated protein aggregates by autophagy. *J. Biol. Chem.* 282:24131–24145.

Rusten, T.E., T. Vaccari, K. Lindmo, L.M. Rodahl, I.P. Nezis, C. Sem-Jacobsen, F. Wendler, J.P. Vincent, A. Brech, D. Bilder, and H. Stenmark. 2007. ESCRTs and Fab1 regulate distinct steps of autophagy. *Curr. Biol.* 17:1817–1825.

Saftig, P., W. Beertsen, and E.L. Eskelinen. 2008. LAMP-2: A control step for phagosome and autophagosome maturation. *Autophagy.* 4:510–512.

Slot, J.W., and H.J. Geuze. 2007. Cryosectioning and immunolabeling. *Nat. Protoc.* 2:2480–2491.

Styers, M.L., A.K. O'Connor, R. Grabski, E. Cormet-Boyaka, and E. Sztul. 2008. Depletion of {beta}-COP reveals a role for COP-I in compartmentalization of secretory compartments and in biosynthetic transport of caveolin-1. *Am. J. Physiol. Cell Physiol.* 294:C1485–C1498.

Tamayo, A.G., A. Bharti, C. Trujillo, R. Harrison, and J.R. Murphy. 2008. COPI coatomer complex proteins facilitate the translocation of anthrax lethal factor across vesicular membranes in vitro. *Proc. Natl. Acad. Sci. USA.* 105:5254–5259.

Tooze, J., M. Hollinshead, T. Ludwig, K. Howell, B. Hoflack, and H. Kern. 1990. In exocrine pancreas, the basolateral endocytic pathway converges with the autophagic pathway immediately after the early endosome. *J. Cell Biol.* 111:329–345.

Whitney, J.A., M. Gomez, D. Sheff, T.E. Kreis, and I. Mellman. 1995. Cytoplasmic coat proteins involved in endosome function. *Cell.* 83:703–713.

Williams, R.L., and S. Urbe. 2007. The emerging shape of the ESCRT machinery. *Nat. Rev. Mol. Cell Biol.* 8:355–368.

Woodman, P.G., and C.E. Futter. 2008. Multivesicular bodies: co-ordinated progression to maturity. *Curr. Opin. Cell Biol.* 20:408–414.

Xie, Z., and D.J. Klionsky. 2007. Autophagosome formation: core machinery and adaptations. *Nat. Cell Biol.* 9:1102–1109.